HHS Public Access

Author manuscript

Plant Mol Biol. Author manuscript; available in PMC 2018 August 08.

Published in final edited form as:

Plant Mol Biol. 2017 November ; 95(4-5): 389–398. doi:10.1007/s11103-017-0657-x.

Papillae formation on trichome cell walls requires the function of the Mediator complex subunit Med25

Christy Fornero, **Bangxia Suo**, **Mais Zahde**, **Katelyn Juveland**, and **Viktor Kirik***

School of Biological Sciences, Illinois State University, Normal, IL 61790, USA

Abstract

The plant cell wall plays an important role in communication, defense, organization and support. The importance of each of these functions varies by cell type. Specialized cells, such as *Arabidopsis* trichomes, exhibit distinct cell wall characteristics including papillae. To better understand the molecular processes important for papillae deposition on the cell wall surface, we identified the *GLASSY HAIR 1 (GLH1)* gene, which is necessary for papillae formation. We found that a splice-site mutation in the component of the transcriptional Mediator complex *MED25* gene is responsible for the near papillae-less phenotype of the *glh1* mutant. The *MED25* gene is expressed in trichomes. Reporters for trichome developmental marker genes *GLABRA2* (*GL2*) and *Ethylene Receptor2* (*ETR2*) were not affected in the *glh1* mutant. Collectively, the presented results show that *MED25* is necessary for papillae formation on the cell wall surface of leaf trichomes and suggest that the *Arabidopsis* MED25 Mediator component is likely involved in the transcription of a subset of genes that promote papillae deposition in trichomes.

Keywords

Cell wall; trichomes; papillae; mediator

Introduction

Plant cell walls play critical roles in cell communication, plant defense, growth, and mechanical support. The *Arabidopsis* leaf trichomes represent an excellent model for studying the mechanisms of cell wall biogenesis and development (Marks at al. 2008). These cells form birefringent, thick cell walls of about 1 μm, which are characteristics typically associated with secondary cell walls. However, trichome cell walls have a biochemical composition more similar to the primary than to the secondary cell wall with a 2.23-fold ratio of pectic to cellulosic sugars (Potika and Delmer 1995; Marks et al. 2008). Even more peculiar, primary *CESA* genes, but not secondary *CESA* genes, are active in *Arabidopsis* trichomes (Jakoby et al. 2008; Marks et al. 2008; Betancur et al. 2010; Lei et al. 2012; Bashline et al. 2014). Such a unique blend of primary and secondary cell wall characteristics make trichomes ideal for studying multiple aspects of cell wall biogenesis and development.

To whom correspondence should be addressed: vmkirik@ilstu.edu, tel: +1-3094382608, fax:: +1-3094383722.

The cell walls of *Arabidopsis* trichomes develop unique structures known as papillae which are raised, rounded subcuticular structures that give the trichome cell surface a bumpy appearance visible under scanning electron microscopy. The functions of *Arabidopsis* trichomes and papillae remain largely unknown. It has been suggested that trichomes may reflect incoming light to prevent water loss, increase drought resistance, and reduce the transmission of harmful Ultra Violet (UV) radiation onto the leaf surface (Karabourniotis et al. 1995; Yan et al. 2012; Polivka & Hofmann 2014). Upon UV-B exposure, *Arabidopsis* trichomes have been shown to increase in number, phenolic content, as well as cell wall thickness (Kulich et al. 2015). As more light gets transmitted through trichomes with reduced papillae (Suo et al. 2013), it is possible that papillae play some role in the proposed protective functions of trichomes,

When viewed under a dissecting microscope, wild type plants exhibit trichomes of a nearly opaque, white color. The frosted appearance of wild type trichomes is believed to be caused by the uneven surface area created by papillae on the surface of the trichome cell wall (Suo et al. 2013). The curved depositions are therefore proposed to scatter light in a similar manner as to that of frosted glass. When papillae are missing or less pronounced, this light scattering property is diminished permitting more light is to pass through the trichome. These trichome cell wall mutants are described as having a more translucent, “glassy” trichome phenotype, compared to the “frosted” trichomes seen in wild type plants.

Although several genetic mutations causing a glassy trichome phenotype have been described, the identities of the genes involved and the molecular mechanism of papillae formation remain largely unknown (Hulskamp et al. 1994; Potikha and Delmer 1995; Jakoby et al. 2008; Bischoff et al. 2010; Suo et al. 2013). The *glassy hair1* mutant possesses trichomes that display a fivefold reduction in papillae density and form undersized, flatter papillae (Suo et al. 2013; Figure 1A). Here we show that the *GLH1* gene encodes the MED25 protein, a component of the transcription Mediator complex. The presented data suggest that papillae formation requires a regulatory step in which the Mediator complex integrates the activity of transcription factors to control the expression of papillae promoting genes.

Results

Mutation in the *MED25* gene causes a glassy trichome phenotype

The *glh1* mutation was previously fine mapped to an interval of 82 kilobases (kb) on the upper arm of *Arabidopsis thaliana’s* chromosome 1 (Suo et al. 2013; Figure 1B). To pursue identification of this gene, it was mapped to the F2J7 BAC. T-DNA insertion lines positioned within the mapping interval were screened for a glassy trichome phenotype. Plants from the SALK_129555c line exhibited a glassy phenotype. The T-DNA insertion for this line disrupts the gene encoding a component of the transcription Mediator complex, *MED25*.

Sequencing of the *MED25* gene in the *glh1* mutant background revealed a Guanine to Adenine substitution at the beginning of the sixth intron (Figure 1C), affecting the splice junction sequence. Such an altered splice junction sequence is likely to cause a splicing

malfunction, which could result in a truncated or extended protein. To test the effects of the mutation on transcript splicing, the cDNA region surrounding the *MED25* mutation site was PCR amplified using primers binding within the fifth and seventh exons. In the reactions on cDNA using *MED25* primers, wild type plants produced a single band of 396bp, while mutant plants produced several bands ranging from approximately 300bp to 600bp (Figure 1D). The presence of multiple bands amplified from the *glh1* mutant cDNA indicates that multiple splice variants are being produced. This also suggests that the identified G to A substitution affected the formation of a functional *GLH1* transcript and greatly reduced or abolished the function of the *GHL1* gene product.

The SALK_129555c T-DNA line (Figure 2C, C′) was crossed with the *glh1* line (Figure 2B, B′) to test for genetic complementation. Analysis of the F1 trichome phenotype revealed that the progeny possessed glassy trichomes with underdeveloped papillae at a low density (Figure 2E, E′), indicating no complementation. To test if the *MED25* gene can rescue the glassy phenotype of *glh1*, the pPZP212 vector containing a genomic fragment with the *MED25* regulatory (1867bp) and coding (5055bp) regions was transformed into the mutant. Trichomes of the T1 generation exhibited frosted appearance and numerous well-developed papillae demonstrating a mutant rescue (Figure 2A, A′; Figure 2D, D′). Papillae density analysis revealed that the *glh1,* SALK_129555c, and *glh1* x SALK_129555c F1 lines possessed significantly fewer papillae than Columbia wild type, whereas the rescued plants showed more papillae than the original *glh1* line (Figure 2F). Collectively, these results established the identity of *GHL1* as *MED25* and indicated that the *glh1* mutation is a new loss-of-function *MED25* allele. Another mutant allele of the Arabidopsis *MED25* gene, describes as *pft1*, was showed delayed flowering time when plants were grown under long-day conditions (Cerdan and Chory 2003). Since the names *GLH1*, *PFT1,* and *MED25* represent the same gene, we will henceforth refer to it as *MED25*.

The *MED25pro::GUS* reporter expresses in trichomes

To determine the localization and relative levels of *MED25* gene expression, the 1867bp fragment of the 5′ regulatory region was used to drive the expression of the β-*glucuronidase (GUS)* reporter. Transgenic plants expressing *MED25pro::GUS* showed reporter activity primarily in leaf vasculature, guard cells, roots, cells surrounding mature trichomes, developing trichomes, and trichomes of young leaves (Figure 3). Fainter staining of trichomes on older leaves was also observed. Consistent with the *MED25pro::GUS* expression, *MED25* transcript has been detected in a trichome microarray analysis (Marks et al. 2009). Together, these results suggest that the *MED25* gene activity in trichome cells promotes papillae formation.

Expression of trichome development reporters is not affected by the *glh1* mutation

To test if the loss of *MED25* function mutation leads to general gene expression defects in trichomes, the expression of two trichome reporters were analysed in the *glh1* mutant. The *GL2* and *ETR2* promoters were shown to be expressed in trichomes during various developmental stages (Szymanski et al. 1998; Plett et al. 2009). *GL2* is important for several stages of trichome development, including cell wall maturation. The *GL2pro::GUS* reporter has been shown to have strong trichome specific expression in leaves (Szymanski et al.

1998; Figure 4). *ETR2* was shown to be important mainly in the early stages of trichome development involving microtubule array stabilization and branch formation (Plett et al. 2009). The F3 generations of the *glh1* x *GL2pro::GUS* and *glh1* x *ETR2pro::GUS* crosses, along with the parental *GUS* lines were stained for GUS activity. No apparent discrepancy in GUS expression between the parental *GUS* and mutant lines was detected in developing or in mature trichomes (Figure 4). These results suggest that the *glh1* mutation does not generally disrupt gene expression in trichomes and that *MED25* may promote papillae deposition by regulating a subset of genes involved in the formation of these structures.

Calcium ion accumulation in trichomes is reduced in the *glh1* mutant trichomes

Previous elemental analyses of the glassy trichome mutants, *gl3-sst* and *gl3-sst sim,* have demonstrated reductions in magnesium, calcium, and phosphorous when comparing mutant and wild type elemental profiles (Esch et al. 2003; Marks et al. 2009). In particular, calcium was suggested to associate with papillae structures (Rerie et al. 1994). An SEM based X-ray elemental analysis was used to determine if the *glh1* mutation affects the elemental composition of the trichome cell wall surface. Analyses were performed on *glh1* trichome cell walls (Figure 5A), Columbia inter-papillae regions (Figure 5B), and Columbia papillae (Figure 5C). A comparison of X-ray peaks from the Columbia inter-papillae and papillae regions revealed no significant differences (Figure 5D). However, a significant reduction in calcium was measured in the *glh1* mutant trichomes (22% of wild type; Figure 5E). Quantitative elemental analysis by Inductively Coupled Plasma Optical Emission Spectroscopy (ICP-OES) showed a significant reduction ($p < 0.001$) of calcium levels to 0.496 ppm per 1,000 trichomes in the *glh1* mutant compared to 1.653 ppm per 1,000 trichomes in wild type (Figure 5F).

Discussion

Transcription of many genes relies on the activity of the Mediator complex, which serves as both an adaptor between specific transcription factors and the promoter-bound RNA polymerase complex, as well as a signal transmitter for transcriptional regulators (Backstrom et al. 2007; Samanta and Thakur 2015). The Mediator complex has additional functions in nuclear processes, regulating miRNA and siRNA biogenesis, D-lop and Holiday structure disruption, RNA processing, and mediating polar nuclei proliferation (Barneche et al. 2000; Yan et al. 2007; Kobbe et al. 2008; Huang et al. 2009; Kang et al. 2009; Maruyama et al. 2010; Kim et al. 2011).

In plants, the Mediator complex has been shown to be involved in various aspects of growth and development, including embryo pattern formation, flowering, organ development, leaf number and size, Synergistic Activation Mediators (SAM) complex organization, ion homeostasis, and lignin biosynthesis (Autran et al. 2002; Clay and Nelson 2005; Gonzalez et al. 2007; Kidd et al. 2009; Gillmor et al. 2010; Ito et al. 2011; Kim et al. 2011; Xu and Li 2012; Sundaravelpandian et al. 2013; Zheng et al. 2013; Bonawitz et al. 2014; Lai et al. 2014; Yang et al. 2014; Zhang et al. 2014; Li et al. 2015). The MED25 subunit has been shown to regulate jasmonate and abscisic acid signaling pathways through interacting with the MYC2 and ABI5 transcription factors. These signaling pathways play integral roles in

mounting defensive and stress responses (Dhawan et al. 2009; Kidd et al. 2009; Chen et al. 2012). *MED25* is also known to be involved in the regulation of flowering time in reaction to light quality, in organ development through the restriction of cell proliferation and expansion, and in repression of Phytochrome B light signaling via interaction with the drought response element binding protein 2A (Xu and Li 2011; Elfving et al. 2011; Inigo et al. 2012). It has therefore been proposed that *MED25* aids in the integration of several different pathways, enabling plants to respond appropriately to various stressors and developmental cues (Malik and Roeder 2010; Elfving et al. 2011; Inigo et al. 2012).

Here, an additional function for the *MED25* gene in trichome papillae formation is demonstrated. Papillae become visible at stages 5 and 6 of trichome development when trichome maturation occurs (Marks et al. 2007). Observed *MED25pro::GUS* expression at early trichome developmental stages suggests either that papillae development may be initiated prior to stage 5, or that *MED25* is also involved in other aspects of early trichome development.

Though the mechanisms of papillae formation and papillae molecular composition are largely unknown, it has long been speculated that these structures may be responsible for the high calcium content found in trichomes (Rerie et al. 1994). Previous analyses of trichome cell wall composition revealed that papillae contain magnesium, calcium, and are enriched in phosphorous (Esch et al. 2003; Marks et al. 2009). Our analysis supports the presence of these elements in papillae though no enrichment was detected in these structures. Analysis of trichome cell wall surfaces and whole trichomes revealed less calcium in the *glh1* mutant compared to wild type. The papillae-less trichomes of the *gl3-sst* mutant were also reported to have decreased calcium levels (Esch et al. 2003). One possibility is that a reduction in calcium may affect papillae formation. Calcium has been suggested to bind and cross-link unmethyl-esterified homogalacturonan pectic polysaccharides, promoting pectin gelation and increasing cell wall stiffening (Caffall and Mohnen, 2009). Reduction in calcium levels in the green alga *Penium margaritaceum* promoted localized cell swelling, illustrating a morphogenetic role of calcium likely due to changes in cell wall structure through pectin cross-linking (Domozych et al., 2014). It is also conceivable that calcium reduction in *glh1* trichomes may merely reflect a reduction in the amount of pectin or changes in its composition. Although hemicellulosic polysaccharides have been previously linked to papillae formation by the fucosyltransferase 1 mutant *mur2* (Vanzin et al., 2002), a possible role of pectin in papillae formation remains to be investigated.

Microarray data from a transcriptome analysis of *Arabidopsis* trichomes (Marks et al. 2009) together with *MED25pro::GUS* expression in leaf trichomes suggest that MED25 is required inside trichome cells to promote papillae formation. Expression of the *GL2pro::GUS* and *ETR2pro::GUS* reporters was not changed in the mutant trichomes, including at the late developmental phases when papillae form. Although it can not be excluded that the papillae-less phenotype of the *glh1* mutant results from trichome developmental arrest, with the *gl3-sst* mutation providing a precedent for this kind of mutation, this scenario seems unlikely since trichome size and shape was shown to be unaffected in the *glh1* mutant (Suo et al. 2013). This suggests an alternative explanation where MED25 is involved in transcription of a subset of trichome-expressed genes that promote papillae formation. MED25 may interact

with the transcription factors necessary for the activation of genes involved in the localized deposition of material on the cell wall surface. Identification of MED25 regulated genes using a trichome-specific transcriptome analysis may provide means to reveal molecular components of the mechanism responsible for papillae deposition on the cell wall surface.

Methods

Plant strains and growth conditions

For aseptic plant growth, plates containing one half Murashige and Skoog (MS) salts with 1% sucrose were used. A soil mixture consisting of one half Promix HP with mycorrhizae (Premier Tech Horticulture Ltd.) and one half Professional Growing Mix (Sun Gro Horticulture Canada Ltd.) was used for plants grown in pots. The mutant *glh1* line was generated by EMS mutagenesis (Suo et al. 2013), the SALK_129555c line was obtained from the Arabidopsis Biological Resource Center, Ohio (http://abrc.osu.edu).

Mapping and identification of the *GLH1* gene

Columbia ecotype mutants were crossed with Landsberg erecta plants. The F2 seeds were grown and tissue samples of mutants were harvested for genomic DNA isolation. Publicly available and newly designed simple length polymorphism (SSLP), cleaved amplified polymorphism (CAP), and derived CAP (dCAP) markers were used for mapping (Meinke et al. 1998; Lukowitz et al. 2000). Once approximately ten recombinants were found for the current set of markers, new markers located inwards in the mapping interval were selected for testing additional samples. This process was repeated until the mapping interval was less than 100kb and nearly all recombinants were lost.

PCRs were performed on wild type and *glh1* mutant genomic DNA to amplify the *MED25* gene in two overlapping fragments using primers S0.1: CAATTTACAAAGAACGAGCTTCA, AS3: TGGGGAAAACTAGGAACTGGTGC, S2: ATCTTCACATTAGTAGAAGCCTG, and AS0: TACCGTCGGCGAATCGTTAGG. The resulting gene fragments were then sequenced to identify the nucleotide mutation. PCRs on wild type and mutant cDNAs were performed using the primers MED25 RT PCR F: GCTCAACCAAGTAACGATCTG and MED25 RT PCR R: CACTTTCACAGGGCTCTGAGT to test the effect of the mutation at the *GLH1* RNA transcript processing. Amplification of the *Elongation Factor 1* cDNA (*EF1*) with primers EF1s: ATGCCCCAGGACATCGTGATTTCAT and EF1as: TTGGCGGCACCCTTAGCTGGATCA, was used as a control.

MED25 gene constructs

The pPZP212 vector containing a genomic fragment including the *MED25* regulatory (1867bp) and coding (5055bp) regions was obtained from Dr. Pablo Cerdan at La Universidad de Buenos Aires, Argentina. To create the *MED25pro::GUS* construct the *MED25* promoter was amplified using the following primers: PROMOTER F2: CTATCGAGCTGGCGATGATGTC and PROMOTER R3: AGTCTCTGAGCGTTGTTGTTACGTG, yielding a product of 1,867bp which was inserted into the pCR8/GW/TOPO vector (Invitrogen). After confirming the sequence, the promoter

fragment was inserted into pMDC162 (Curtis and Grossniklaus 2003) to obtain the *MED25pro::GUS* construct.

GUS staining and microscopy

The GUS staining solution was prepared as described in Xu and Li 2011. Ten-day-old seedlings were incubated at 37 °C overnight. Afterward, the GUS staining solution was removed and 70% ETOH was added to preserve samples and extract chlorophyll. Light microscopy images were documented using a Leica CCD camera.

Leaves three, four, and five of three-week-old plants were used for all scanning electron microscope (SEM) images. The SEM images in Figure 1 were taken using the low vacuum mode setting on the FEI Quanta 450 scanning electron microscope as described in Suo et al. 2013. For the SEM images in Figure 2, plant tissue was prepared via primary fixation in a 4% glutaraldehyde-phosphate buffer solution. After two hours, the primary fixative was removed and the plant tissue was rinsed three times with phosphate buffer, ten minutes per wash. A secondary fixation was carried out using a 1% osmium tetroxide-phosphate buffer solution. The secondary fixative was removed after one hour and the plant tissue was rinsed as before. Samples were then dehydrated via ten minute incubations in increasing concentrations of ETOH: 10%, 30%, 50%, 70%, 95%, 100%, 100%, 100%. The samples were subjected to critical point drying, mounted on stubs, and sputter coated with gold for four minutes. Images were taken using the high vacuum mode setting on the FEI Quanta 450 scanning electron microscope. Trichomes were viewed using 500x and 1000x magnification, a pressure of approximately 2.99e-6 Torr, a voltage of 12.5–15kV, and a spot size of 3.0.

Papillae quantification

High vacuum scanning electron images of trichomes taken at 1000x magnification. Papillae were counted within a 200px x 300px (24.84 μm × 37.50 μm) rectangular region on the trichome base. was used to define a region on the trichome base within which. Two-tailed two-sample t-tests were performed to compare measurements.

X-ray elemental analysis

Trichomes were viewed using the high vacuum mode setting on the FEI Quanta 450 scanning electron microscope at 5000x magnification. X-ray analysis was performed using a $1\mu m^2$ region of interest for approximately 2,000 frames per sample using an X-MAX silicon drift detector and INCA software (Oxford Instruments). Analyses were performed on *glh1* trichome cell walls, Columbia inter-papillae regions, and Columbia papillae. Once spectra were acquired for mutant and wild type trichomes, peak heights were measured for calcium. Two-tailed two-sample t-test was performed to compare the elemental make-up of wild type and mutant trichome cell wall surfaces.

ICP elemental analysis

Trichomes were isolated as described in Marks *et al* 2008. Isolated trichomes were re-suspended in approximately 10 ml PBS (potassium salts only). Six aliquots of 5 μl were removed for cell counts to determine trichome concentration. Aliquots of approximately 3,000 trichomes were distributed into vials and buffer was aspirated. Each vial of trichomes

was prepared for ICP analysis by adding 0.5 ml of concentrated nitric acid, 0.5 ml concentrated hydrochloric acid, and 9.0 ml of nanopure water.

Thirteen standards ranging from 0.01 ppm to 15.0 ppm were prepared using the ICCA VeriSpec Instrument Calibration Standard 5 stock solution (1,000 ppm). For each standard, a given volume of stock solution was diluted with 5.0 ml concentrated nitric acid, 5.0ml concentrated hydrochloric acid, and nanopure water up to 100ml.

Standards and samples were run on an Optima 8300 ICP-OES Optical Emission Spectrometer produced by Perkin Elmer. The program Syngistix for ICP was used in conjunction with the spectrometer to process the results. The read parameters were set to auto, with a delay time of 45 sec, and 3 replicates. The Perkin Elmer blank solution was ran prior to standards and samples to determine background signal. Sample intensity values were recorded for the calcium 315.887 nm and calcium 393.366 nm emission wavelengths and exported to Microsoft Excel for data analysis. Corrected intensities were calculated by subtracting the blank intensity value from the standard and sample intensity values. A standard curve was generated by plotting the corrected standard intensities against the standard concentrations. Using the equation for the linear regression line, the concentration of calcium was calculated for each sample. A two-tailed two-sample t-test was performed to compare calcium concentrations between wild type and mutant samples.

Acknowledgments

The authors would like to thank Stephanie Seifert for her help with the genetic mapping of the *GLH1* gene. Thanks are due to the Arabidopsis Biological Resource Center (http://abrc.osu.edu), from which we obtained T-DNA lines. We would like to acknowledge Dr. Pablo Cerdan for sending us the pPZP212 vector containing the *MED25* regulatory and coding regions (Inigo et al 2012), and Dr. Sharon Regan at Queen's University, Ontario Canada, for sending us *ETR2pro::GUS* lines (Plett et al. 2009). We also extend our appreciation to Dr. Martha Cook for her help with the SEM imaging and to Dr. Jun-Hyun Kim and Tony Ludwig for their help with the ICP analysis. This research was supported by Illinois State University (CF, BS, and VK) and by a Weigel Grant from the Beta Lambda chapter of Phi-Sigma Biological Society to CF.

References

Autran D, Jonak C, Belcram K, Beemster GT, Kronenberger J, Grandjean O, Inzé D, Traas J. Cell numbers and leaf development in *Arabidopsis*: a functional analysis of the STRUWWELPETER gene. EMBO J. 2002; 21:6036–6049. [PubMed: 12426376]

Bäckström S, Elfving N, Nilsson R, Wingsle G, Björklund S. Purification of a plant mediator from *Arabidopsis thaliana* identifies PFT1 as the MED25 subunit. Mol Cell. 2007; 26:717–729. [PubMed: 17560376]

Barneche F, Steinmetz F, Echeverría M. Fibrillarin genes encode both a conserved nucleolar protein and a novel small nucleolar RNA involved in ribosomal RNA methylation in *Arabidopsis thaliana*. J Biol Chem. 2000; 275:27212–27220. [PubMed: 10829025]

Bashline L, Li S, Gu Y. The trafficking of the cellulose synthase complex in higher plants. Ann Bot. 2014; 114:1059–1067. [PubMed: 24651373]

Betancur L, Singh B, Rapp RA, Wendel JF, Marks MD, Roberts AW, Haigler CH. Phylogenetically distinct cellulose synthase genes support secondary cell wall thickening in *Arabidopsis* shoot trichomes and cotton fiber. J Integr Plant Biol. 2010; 52:205–220. [PubMed: 20377682]

Bischoff V, Nita S, Neumetzler L, Schindelasch D, Urbain A, Eshed R, Persson S, Delmer D, Scheible WR. TRICHOME BIREFRINGENCE and its homolog AT5G01360 encode plant-specific DUF231 proteins required for cellulose biosynthesis in *Arabidopsis*. Plant Physiol. 2010; 153:590–602. [PubMed: 20388664]

Bonawitz ND, Kim JI, Tobimatsu Y, Ciesielski PN, Anderson NA, Ximenes E, Maeda J, Ralph J, Donohoe BS, Ladisch M, Chapple C. Disruption of Mediator rescues the stunted growth of a lignin-deficient *Arabidopsis* mutant. Nature. 2014; 509:376–380. [PubMed: 24670657]

Caffall KH, Mohnen D. The structure, function, and biosynthesis of plant cell wall pectic polysaccharides. Carbohydrate Research. 2009; 344:1879–1900. [PubMed: 19616198]

Cerdán PD, Chory J. Regulation of flowering time by light quality. Nature. 2003; 423:881–885. [PubMed: 12815435]

Chen R, Jiang H, Li L, Zhai Q, Qi L, Zhou W, Liu X, Li H, Zheng W, Sun J, Li C. The *Arabidopsis* mediator subunit MED25 differentially regulates jasmonate and abscisic acid signaling through interacting with the MYC2 and ABI5 transcription factors. Plant Cell. 2012; 24:2898–2916. [PubMed: 22822206]

Clay NK, Nelson T. The recessive epigenetic swellmap mutation affects the expression of two step II splicing factors required for the transcription of the cell proliferation gene STRUWWELPETER and for the timing of cell cycle arrest in the *Arabidopsis* leaf. Plant Cell. 2005; 17:1994–2008. [PubMed: 15937226]

Curtis MD, Grossniklaus U. A gateway cloning vector set for high-throughput functional analysis of genes in planta. Plant Physiol. 2003; 133:462–469. [PubMed: 14555774]

Dhawan R, Luo H, Foerster AM, Abuqamar S, Du HN, Briggs SD, Mittelsten Scheid O, Mengiste T. HISTONE MONOUBIQUITINATION1 interacts with a subunit of the mediator complex and regulates defense against necrotrophic fungal pathogens in *Arabidopsis*. Plant Cell. 2009; 21:1000–1019. [PubMed: 19286969]

Domozych DS, Sørensen I, Popper ZA, Ochs J, Andreas A, Fangel JU, Pielach A, Sachs C, Brechka H, Ruisi-Besares P, Willats WG, Rose J. Pectin metabolism and assembly in the cell wall of the charophyte green alga *Penium margaritaceum*. Plant Physiol. 2014; 165:105–118. [PubMed: 24652345]

Esch JJ, Chen M, Sanders M, Hillestad M, Ndkium S, Idelkope B, Neizer J, Marks MD. A contradictory GLABRA3 allele helps define gene interactions controlling trichome development in *Arabidopsis*. Development. 2003; 130:5885–94. [PubMed: 14561633]

Elfving N, Davoine C, Benlloch R, Blomberg J, Brännström K, Müller D, Nilsson A, Ulfstedt M, Ronne H, Wingsle G, Nilsson O, Björklund S. The *Arabidopsis thaliana* MED25 mediator subunit integrates environmental cues to control plant development. PNAS. 2011; 108:8245–8250. [PubMed: 21536906]

Gillmor CS, Park MY, Smith MR, Pepitone R, Kerstetter RA, Poethig RS. The MED12-MED13 module of Mediator regulates the timing of embryo patterning in *Arabidopsis*. Development. 2010; 137:113–122. [PubMed: 20023166]

Gonzalez D, Bowen AJ, Carroll TS, Conlan RS. The transcription corepressor LEUNIG interacts with the histone deacetylase HDA19 and Mediator components MED14 (SWP) and CDK8 (HEN3) to repress transcription. Mol Cell Biol. 2007; 27:5306–5315. [PubMed: 17526732]

Hatfield RD, Ralph J, Grabber JH. Cell wall cross-linking by ferulates and diferulates in grasses. J Sci Food Agric. 1999; 79:403–407.

Huang L, Jones AM, Searle I, Patel K, Vogler H, Hubner NC, Baulcombe DC. An atypical RNA polymerase involved in RNA silencing shares small subunits with RNA polymerase II. Nat Struct Mol Biol. 2009; 16:91–93. [PubMed: 19079263]

Hülskamp M, Misŕa S, Jürgens G. Genetic dissection of trichome cell development in *Arabidopsis*. Cell. 1994; 76:555–566. [PubMed: 8313475]

Iñigo S, Alvarez MJ, Strasser B, Califano A, Cerdán PD. PFT1, the MED25 subunit of the plant mediator complex, promotes flowering through CONSTANS dependent and independent mechanisms in *Arabidopsis*. Plant J. 2012; 69:601–612. [PubMed: 21985558]

Ito J, Sono T, Tasaka M, Furutani M. MACCHI-BOU 2 is required for early embryo patterning and cotyledon organogenesis in *Arabidopsis*. Plant Cell Physiol. 2011; 52:539–552. [PubMed: 21257604]

Jakoby MJ, Falkenhan D, Mader MT, Brininstool G, Wischnitzki E, Platz N, Hudson A, Hülskamp M, Larkin J, Schnittger A. Transcriptional profiling of mature *Arabidopsis* trichomes reveals that

NOECK encodes the MIXTA-like transcriptional regulator MYB106. Plant Physiol. 2008; 148:1583–1602. [PubMed: 18805951]

Kang CH, Feng Y, Vikram M, Jeong IS, Lee JR, Bahk JD, Yun DJ, Lee SY, Koiwa H. Arabidopsis thaliana PRP40s are RNA polymerase II Cterminal domain-associating proteins. Arch Biochem Biophys. 2009; 484:30–38. [PubMed: 19467629]

Karabourniotis G, Kotsabassidis D, Manetas Y. Trichome density and its protective potential against ultraviolet-B radiation-damage during leaf development. Canadian Journal of Botany. 1995; 75:376–383.

Kidd BN, Edgar CI, Kumar KK, Aitken EA, Schenk PM, Manners JM, Kazan K. The mediator complex subunit PFT1 is a key regulator of jasmonate-dependent defense in *Arabidopsis*. Plant Cell. 2009; 21:2237–2252. [PubMed: 19671879]

Kim YJ, Zheng B, Yu Y, Won SY, Mo B, Chen X. The role of Mediator in small and long noncoding RNA production in *Arabidopsis thaliana*. EMBO J. 2011; 30:814–822. [PubMed: 21252857]

Kobbe D, Blanck S, Demand K, Focke M, Puchta H. AtRECQ2, a RecQ helicase homologue from *Arabidopsis thaliana*, is able to disrupt various recombinogenic DNA structures in vitro. Plant J. 2008; 55:397–405. [PubMed: 18419780]

Kulich I, Vojtíková Z, Glanc M, Ortmannová J, Rasmann S, Žárský V. Cell wall maturation of *Arabidopsis* trichomes is dependent on exocyst subunit EXO70H4 and involves callose deposition. Plant Phys. 2015; 168:120–131.

Lai Z, Schluttenhofer CM, Bhide K, Shreve J, Thimmapuram J, Lee SY, Yun DJ, Mengiste T. MED18 interaction with distinct transcription factors regulates multiple plant functions. Nature Commun. 2014; 5:3064.doi: 10.1038/ncomms4064 [PubMed: 24451981]

Lei L, Li S, Gu Y. Cellulose synthase complexes: composition and regulation. Front Plant Sci. 2012; 3:75.doi: 10.3389/fpls.2012.00075 [PubMed: 22639663]

Li W, Yoshida A, Takahashi M, Maekawa M, Kojima M, Sakakibara H, Kyozuka J. SAD1, an RNA polymerase I subunit A34.5 of rice, interacts with Mediator and controls various aspects of plant development. Plant J. 2015; 81:282–291. [PubMed: 25404280]

Lukowitz W, Gillmor CS, Scheible WR. Positional cloning in *Arabidopsis*. Why it feels good to have a genome initiative working for you. Plant Phys. 2000; 123:795–805.

Malik S, Roeder RG. The Metazoan Mediator co-activator complex as an integrative hub for transcriptional regulation. Nat Rev Genet. 2010; 11:761–772. [PubMed: 20940737]

Marks MD, Betancur L, Gilding E, Chen F, Bauer S, Wenger JP, Dixon RA, Haigler CH. A new method for isolating large quantities of *Arabidopsis* trichomes for transcriptome, cell wall and other types of analyses. Plant J. 2008; 56:483–492. [PubMed: 18643981]

Marks MD, Gilding E, Wenger JP. Genetic interaction between glabra3-shapeshifter and siamese in *Arabidopsis thaliana* converts trichome precursors into cells with meristematic activity. Plant J. 2007; 52:352–361. [PubMed: 17764505]

Marks MD, Wenger JP, Gilding E, Jilk R, Dixon RA. Transcriptome analysis of *Arabidopsis* wild-type and *gl3–sst sim* trichomes identifies four additional genes required for trichome development. Mol Plant. 2009; 2:803–822. [PubMed: 19626137]

Maruyama D, Endo T, Nishikawa S. BiP-mediated polar nuclei fusion is essential for the regulation of endosperm nuclei proliferation in *Arabidopsis thaliana*. PNAS. 2010; 107:1684–1689. [PubMed: 20080634]

Meinke DW, Cherry JM, Dean C, Rounsley SD, Koornneef M. *Arabidopsis thaliana*: a model plant for genome analysis. Science. 1998; 282:662–682. [PubMed: 9784120]

Plett JM, Mathur J, Regan S. Ethylene receptor ETR2 controls trichome branching by regulating microtubule assembly in *Arabidopsis thaliana*. J Exp Bot. 2009; 60:3923–3933. [PubMed: 19648171]

Polivka T, Hofmann E. The structural basis of biological energy generation. Hohmann-Marriott Martin F, editorSpringer; 2014.

Potikha T, Delmer DP. A mutant of *Arabidopsis thaliana* displaying altered patterns of cellulose deposition. Plant J. 1995; 7:453–460.

Rerie WG, Feldmann KA, Marks MD. The GLABRA2 gene encodes a homeodomain protein required for normal trichome development in *Arabidopsis*. Genes Dev. 1994; 8:1388–1399. [PubMed: 7926739]

Samanta S, Thakur JK. Importance of Mediator complex in the regulation and integration of diverse signaling pathways in plants. Front Plant Sci. 2015; 6:757.doi: 10.3389/fpls.2015.00757 [PubMed: 26442070]

Suo B, Seifert S, Kirik V. *Arabidopsis GLASSY HAIR* Genes Promote Trichome Papillae Development. J Exp Bot. 2013; 64:4981–4991. [PubMed: 24014871]

Sundaravelpandian K, Chandrika NN, Schmidt W. PFT1, a transcriptional Mediator complex subunit, controls root hair differentiation through reactive oxygen species (ROS) distribution in *Arabidopsis*. New Phytol. 2013; 197:151–161. [PubMed: 23106228]

Szymanski DB, Jilk RA, Pollock SM, Marks MD. Control of *GL2* expression in *Arabidopsis* leaves and trichomes. Development. 1998; 125:1161–1171. [PubMed: 9477315]

Vanzin GF, Madson M, Carpita NC, Raikhel NV, Keegstra K, Reiter WD. The *mur2* mutant of *Arabidopsis thaliana* lacks fucosylated xyloglucan because of a lesion in fucosyltransferase AtFUT1. PNAS. 2002; 99:3340–3345. [PubMed: 11854459]

Xu R, Li Y. Control of final organ size by mediator complex subunit 25 in *Arabidopsis thaliana*. Development. 2011; 138:4545–4554. [PubMed: 21903673]

Xu R, Li Y. The Mediator complex subunit 8 regulates organ size in *Arabidopsis thaliana*. Plant Signal Behav. 2012; 7:182–183. [PubMed: 22353872]

Yan A, Pan J, An L, Gan Y, Feng H. The responses of trichome mutants to enhanced ultraviolet-B radiation in *Arabidopsis thaliana*. J Photochem Photobiol B. 2012; 113:29–35. [PubMed: 22647943]

Yan D, Zhang Y, Niu L, Yuan Y, Cao X. Identification and characterization of two closely related histone H4 arginine 3 methyltransferases in *Arabidopsis thaliana*. Biochem J. 2007; 408:113–121. [PubMed: 17666011]

Yang Y, Ou B, Zhang J, Si W, Gu H, Qin G, Qu LJ. The *Arabidopsis* Mediator subunit MED16 regulates iron homeostasis by associating with EIN3/EIL1 through subunitMED25. Plant J. 2014; 77:838–851. [PubMed: 24456400]

Zhang Y, Wu H, Wang N, Fan H, Chen C, Cui Y, Liu H, Ling HQ. Mediator subunit 16 functions in the regulation of iron uptake gene expression in *Arabidopsis*. New Phytol. 2014; 203:770–783. [PubMed: 24889527]

Zheng Z, Guan H, Leal F, Grey PH, Oppenheimer DG. Mediator subunit18 controls flowering time and floral organ identity in *Arabidopsis*. PLoS ONE. 2013; 8:e53924.doi: 10.1371/journal.pone.0053924 [PubMed: 23326539]

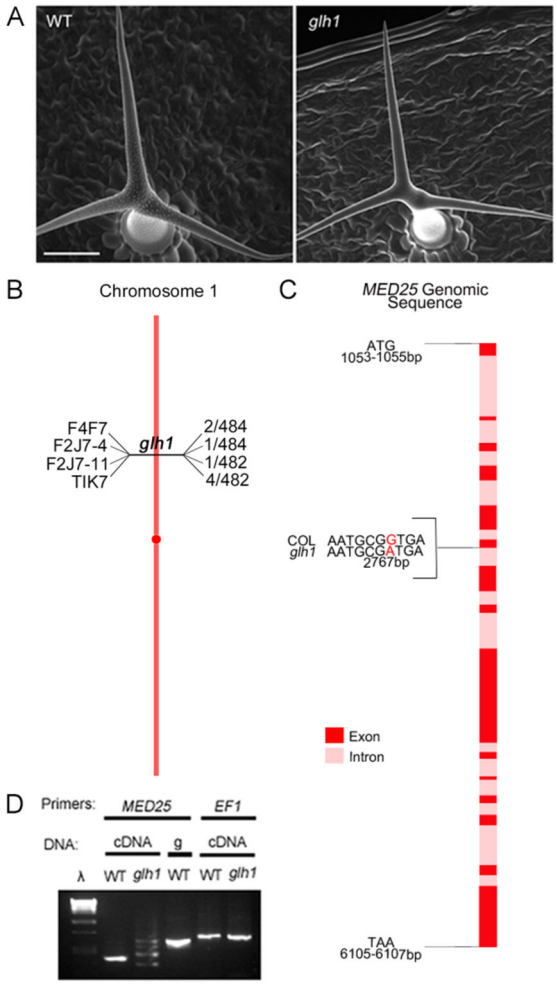

Figure 1. *GLH1* Gene Identification

A. The *glh1* phenotype. In comparison to wild type plants, *glassy hair1* mutants possess trichomes with a low density of underdeveloped papillae on their cell wall surfaces. Scale bar=75μm.

B. *glh1* Mutation Mapping Interval. The g*lh1* mutation was mapped to an 82kb region on chromosome 1. The names of the markers and the number of recombinants in relation to the number of chromosomes tested are indicated.

C. Mutation Location. *MED25* was sequenced in the *glh1* background and aligned with wild type Columbia sequences, revealing a point mutation at the beginning of the sixth intron that resulted in a Guanine to Adenine substitution.

D. Mutation Effects on Transcript Splicing. PCR amplification of Arabidopsis *MED25* cDNA using *MED25* primers yielded a single band of 396bp for wild type plants and several bands ranging from approximately 300bp to 600bp for mutant plants. The PCR on wild type genomic DNA (g) using *MED25* primers generated a single band of 634bp in length. Reactions on cDNA using *EF1* primers was used as a control.

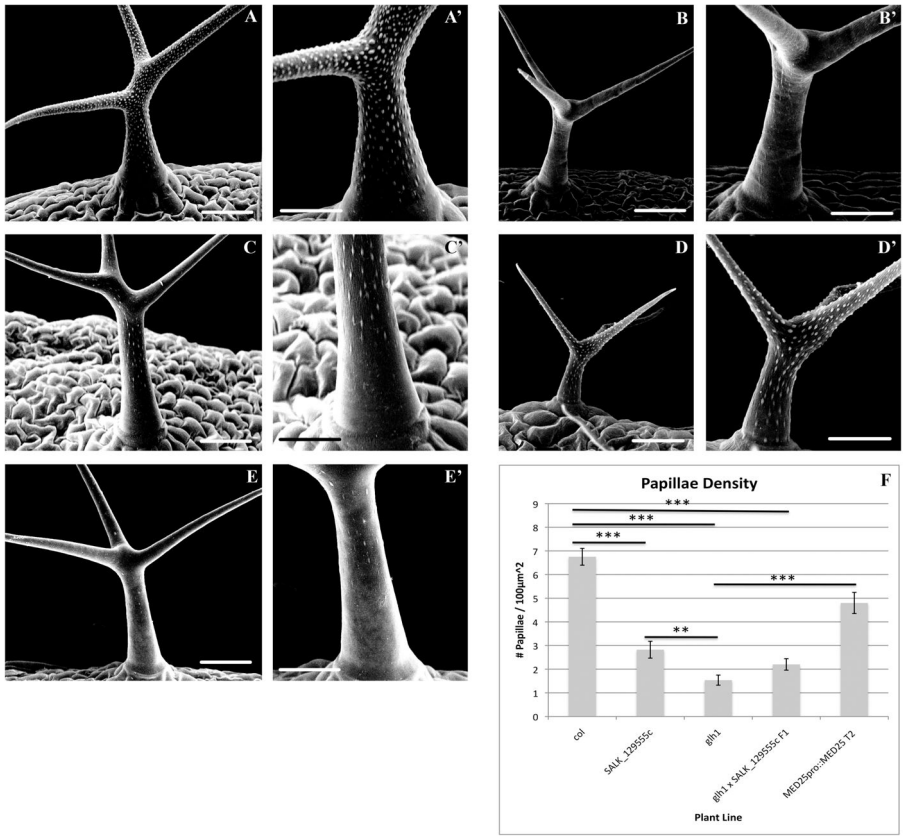

Figure 2. Complementation of the *glh1* mutant

A–E. Scanning electron micrographs of whole trichomes at 500x magnification. Scale bars = 50µm. A′–E′ Scanning electron micrographs of trichome stalks at 1000x magnification. Scale bars = 30µm.

A, A′. Wild type trichomes possess numerous fully formed papillae.

B, B′. *glh1* trichomes exhibit underdeveloped papillae at a dramatically reduced density compared to wild type.

C, C′. SALK_129555c trichomes have underdeveloped papillae at a reduced density compared to wild type.

D, D′. Trichomes of the *glh1* mutants expressing *MED25pro::MED25 construct* display numerous fully developed papillae.

E, E′. SALK_129555c x *glh1* F1 trichomes possess underdeveloped papillae at a dramatically reduced density compared to wild type.

F. Density of Papillae for *glh1*, Columbia, SALK_129555c, SALK_129555c x *glh1* F1, and *MED25pro::MED25* T2 trichomes. N=13 for *glh1*, N=10 for all other plant lines, **=P<0.01, ***=P<0.001.

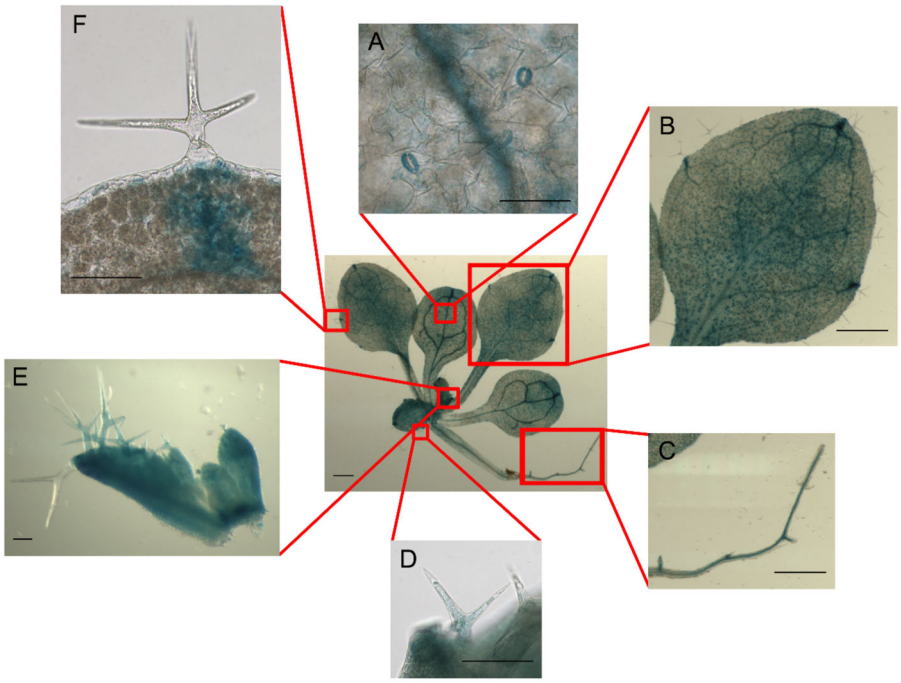

Figure 3. Expression of the *MED25pro::GUS* in Seedlings

GUS staining in ten-day-old seedlings was evident primarily in A guard cells, B leaf vasculature, C roots, D developing trichomes, E trichomes of young leaves, and F cells surrounding mature trichomes. For A, D, E, F scale bars=100μm, for B and C scale bars=1 mm.

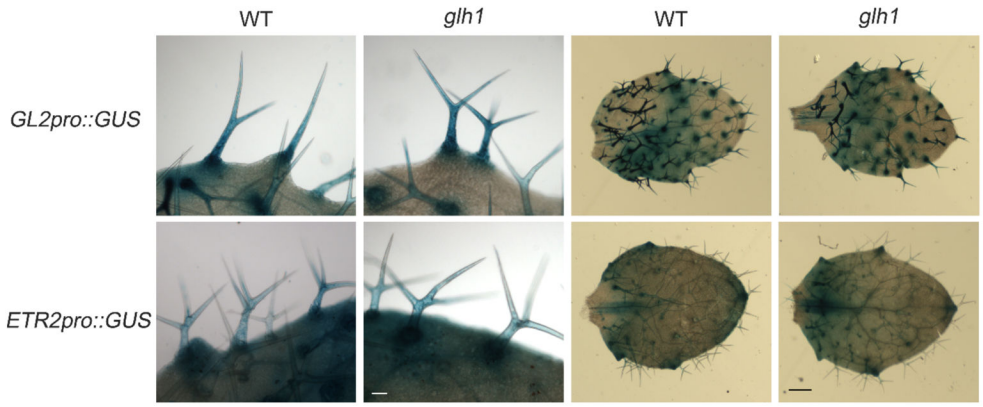

Figure 4. *GL2pro::GUS* and *ETR2pro::GUS* Expression in the *glh1* Trichomes

Trichome and whole leaf images are shown for each parental and F3 line. Scale bar for trichome images=50μm. Scale bar for leaf images= 200μm.

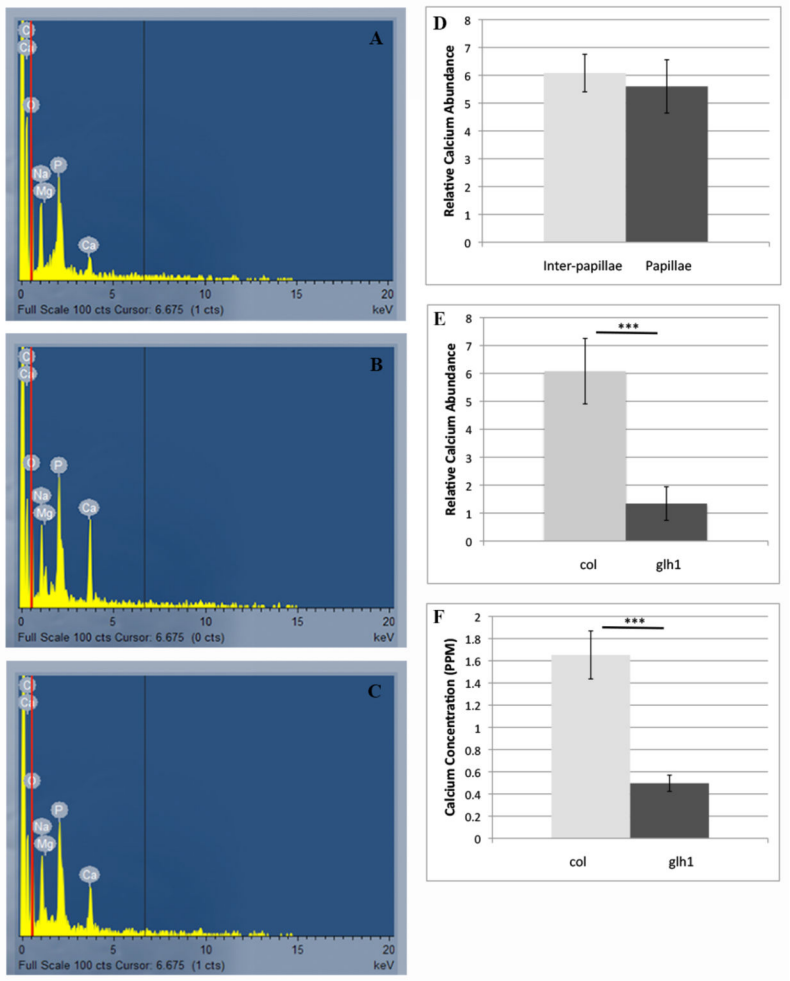

Figure 5. Trichome Elemental Analysis

X-ray peaks for *glh1* trichome surfaces (A), wild type inter-papillae regions (B), and wild type papillae (C) were measured to compare the elemental composition of wild type and mutant trichome cell wall surfaces. No significant differences in calcium were detected between X-ray peaks from the Columbia inter-papillae and Columbia papillae regions (D). Comparisons of X-ray peak heights (E) and ICP ppm values (F) between Columbia and *glh1* samples revealed that mutant trichomes contain less calcium. N=5 trichomes for each plant line used in the X-ray dispersal spectra analysis. N=14 vials (3000 trichomes per vial) for each plant line used in the ICP analysis. *=P<0.05, **=P<0.01, ***=P<0.001.